Jestr

Journal of Engineering Science and Technology Review 16 (4) (2023) 188 - 195

Research Article

JOURNAL OF
Engineering Science and Technology Review

www.jestr.org

Tilt Angle Optimization of Steam Turbine Blade Model Based on Aluminium: The Multi-Simulation Perspective

Ariyana Dwiputra Nugraha[1], Muhamad Kevin Fajrin[2], Zeeshan Hamid Malik[2], Jayan Sentanuhady[2], Muhammad Kusni[3], Seno Darmanto[4], Benny Sutanto[1], Gesang Nugroho[2] and Muhammad Akhsin Muflikhun[2,*]

[1]*PLN Research Institute, Jakarta, Indonesia*
[2]*Mechanical and Industrial Engineering Department, Gadjah Mada University, Yogyakarta, Indonesia.*
[3]*Bandung Institute of Technology, Bandung, Indonesia*
[4]*Diponegoro University, Semarang, Indonesia*

Received 25 February 2023; Accepted 8 September 2023

Abstract

Turbine blades are radial aerofoils attached to the rim of a turbine rotor to generate tangential force that helps to harvest energy from high-pressure steam. The more energy extracted, the more efficient the turbine and the more power produced. The blade's profile, tip and root are the crucial parts of a steam turbine blade. This research analyses the varying tilt angles of a steam turbine blade composed of aluminium alloy using a NACA 4412 aerofoil. Three types of simulations have been implemented; static structural, steady state thermal and fluent analysis, to determine the optimal tilt angle. In static structural analysis the lowest total deformation of 0.33 mm, minimum stress of 33.16 MpA and least stain of 0.52 mm/min occurred at a tilt angle of 35° of turbine blade. Whereas steady state thermal analysis records the total heat flux of 1.55E+08 (W/m^2) at 35°. The fluent analysis determined the lift, drag, pressure average, and velocity of air at a twist angle of 35° to be 507.65 N, 170.16 N, 26.19 kPa, and 383.97 m/s, respectively. The results suggested that for optimum performance, an aluminium alloy stream turbine blade should be tilted at a 35° angle. Aluminium Metal Matrix Composite have improved corrosion resistance with introduction of second phase particles and light weight structure will be more energy efficient.

Keywords: Design of turbine blade, Modelling and Simulation, Tilt angle Optimization, Novel Aluminium blade, Structural and Fluent Analysis

1. Introduction

Turbine is one of the core equipment of the generation system where the turbine functions to generate mechanical energy in the form of rotation by utilizing the driving fluid [1], [2]. This driving fluid produces torque so that the turbine can rotate, the force exerted by the fluid (steam) with a certain enthalpy can create the large torque needed to rotate the turbine at high speed [3]–[5]. The turbine can rotate by utilizing the kinetic energy [6] of steam provided by the driving energy. The turbine referenced in this paper is a steam turbine. [7], [8]. It is well known that steam turbines currently provide the majority of the world's power [9], [10]. There is an increasing necessity for the steam turbine to handle the role of peak-load management since the solar [11] and wind power [12] plants are rarely available to regulate the load on networks. As peak-load on grids falls, the steam turbine normally runs in an off-rated mode [13], with a substantially lower mass-flow rate of steam than in the rated condition. When mass flow rate decreases, the work capacity of turbine blades likewise decreases [14], lowering system performance and safety. The aerodynamic performance and energy efficiency [15] of steam turbine must thus be improved, especially when operating with low mass flow rates. Steam Turbine consists of several blades arranged in series, and each blade has various characteristics in their working principle. Turbine blades are the primary component of a gas turbine [16], [17] or steam turbine's section. These turbine blades are responsible for extracting energy [18] from the high temperature [19], high pressure gases [20] produced by the combustion chamber [4,18–20].

A turbine blade's aerodynamic [24] profile must be carefully considered in order to the steam flow properly and produce rotational energy effectively. Turbine blades must also be sturdy enough to endure high centrifugal pressures and be sized to minimize unwanted vibrations. Many types of turbine blades have been suggested, but practically all of them are built to benefit from the idea that when a mass of steam abruptly changes its velocity, the mass will produce a force that is directly proportional to the rate of change of velocity [25], [26]. Steam Turbine blades consist of various components, namely blade tip, blade profile, and blade root. In the Turbine Blade, the Blade Profile [27] is consisting of convex surface [28] which known as the back arc, a concave surface [29] known as the inner arc, and the transition part between the convex and concave surfaces which are both known as the leading edge [30] and trailing edge [31]. The Blade Root [32] is the component on the Turbine Blade that is in direct contact with the hub, and the Blade Tip [33] is the component on the Turbine Blade that is furthest from the hub.

Aluminium has been extensively used in applications, which include military engineering, aerospace and transportation industries where properties such as attractive appearance, lightweight, excellent corrosion resistance and

*E-mail address: akhsin.muflikhun@ugm.ac.id
ISSN: 1791-2377
doi:10.25103/jestr.164.23

good strength are paramount. The properties of aluminium can, however, be improved despite its unique attributes through the introduction of second-phase particle(s) into the matrix [15]. This could be achieved through the introduction of any or a combination of metallics, ceramics, nitrides, nanoceramics or agro-based waste to the aluminium matrix, thereby leading to the formation of aluminium matrix composites (AMCs) [34].

The design of a steam turbine blade may be improved in a number of ways, but in this study, static structural, steady state thermal, and fluent analysis simulations have been implemented to analyse the varying tilt angles of a steam turbine blade composed of aluminium alloy using a NACA 4412 aerofoil to find the optimal performance and sustainable manufacturing. The following blade tilt angles have been simulated: 33°, 34°, 35°, 36°, 37°, and 38°.

2. Simulation Methods

There are a few things to undertake in order to improve the outcome of the steam turbine blade's simulation. The first step is to do research on the properties and calculations of steam turbine blades. After acquiring desired parameters proceed with the design, fulfil the simulations requirements to get optimal results. It is further simplified as follows.

2.1. Doing Research about Steam Turbine Blade

Researching the parameters or calculations for designing a steam turbine is essential in order to develop a good design. This study is a critical stage since it provides us with numerous calculations for developing a suitable steam turbine design. To provide a better computation for the design of the steam turbine blade, a number of calculations should be employed. The calculations and relevant perimeters have been further classified in to the following:

2.1.1. Airfoil Selection

Since it may create lift, drag, and moment on the turbine blade, the airfoil or aerofoil is a crucial component. To achieve the best results, utilize an airfoil that is commonly used in industry. NACA Air tools ought to be used to design the optimal airfoil for a steam turbine blade.

2.1.2. Material Selection

Many variables, such as the turbine design, operating circumstances, and application requirements, influence the material choice for steam turbine blades. Nonetheless, the following materials are frequently used for steam turbine blades:

- High-Strength Steel: Low-alloy steels such as ASTM A723 and ASTM A387 are often used for high-pressure steam turbine blades. They possess exceptional resistance to high-temperature creep, high tensile strength, and good toughness.
- Nickel-based superalloys, such as Inconel 718 and Inconel 738, are utilized in both low-pressure and high-pressure steam turbine blades. They have exceptional high-temperature strength, creep resistance, and corrosion resistance.
- Titanium-based Alloys: Low-pressure steam turbine blades frequently employ titanium alloys like Ti-6Al-4V and Ti-6Al-2Sn-4Zr-2Mo. They offer a high strength-to-weight ratio, great corrosion resistance, and strong creep resistance.
- Ceramic Matrix Composites: Innovative materials such as ceramic matrix composites (CMCs) are becoming more widespread in steam turbine blades. They offer exceptional high-temperature strength and thermal shock resistance, which helps boost steam turbine efficiency.

The novelty of this study is to analyse the varying tilt angles of a steam turbine blade composed of aluminium alloy using a NACA 4412 aerofoil to find the optimal performance.

2.1.3. Centrifugal Force

Centrifugal forces in general can be expressed as;

$$F = mr\omega^2 \quad (1)$$

where

F = Centrifugal Force
m = Mass of the moving object
r = Distance of object from centre of rotation
ω = Angular Velocity

For this case, in steam turbine blade for centrifugal force can be expressed in Equation 2.

$$F = \rho A\omega^2 \int_{r2}^{r1} r dr \quad (2)$$

Where ρ is density material and A is cross blade section

This formula is used to get a better result for steam turbine blade design. Please refer Table 1

Table 1. Calculation design for steam turbine blade

Material	Aluminium Alloy
Density	7850 kg/m^3
Airfoil	NACA 4412
Cross Sectional Area	727,827 mm2
Blade Tip	96 mm
Blade Root	100 mm
Blade Length	200 mm
Centrifugal Force	78738,37 N

2.1.4. Steam Turbine Blade Design

After obtaining the optimum calculations steam turbine blade is designed using CAD (Computer Aided Design). There are multiple applications to make CAD design, in this case the Autodesk Inventor is used for designing. The design is as follows.

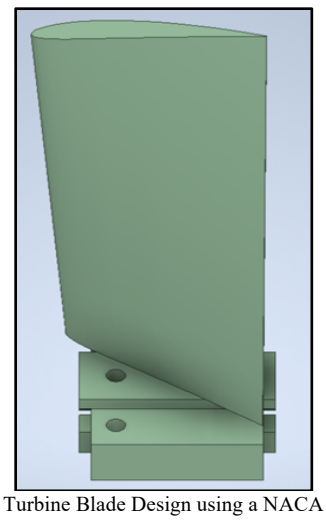

Fig. 1. 3D Steam Turbine Blade Design using a NACA 4412 aerofoil

Considering the twist angle of blade, six different turbine blades are designed for simulation. Twist angle of steam turbine blade is the angle between the Blade Tip and Blade Root. To obtain this angle, an isometric design of the turbine blade is perceived from top. A line is then drawn between the airfoils, and finally, the turbine blade's twist angle is determined. The referenced twist angles range from 33 to 38 degrees[35]. On the basis of varying twist angles, the engineering design is shown below.

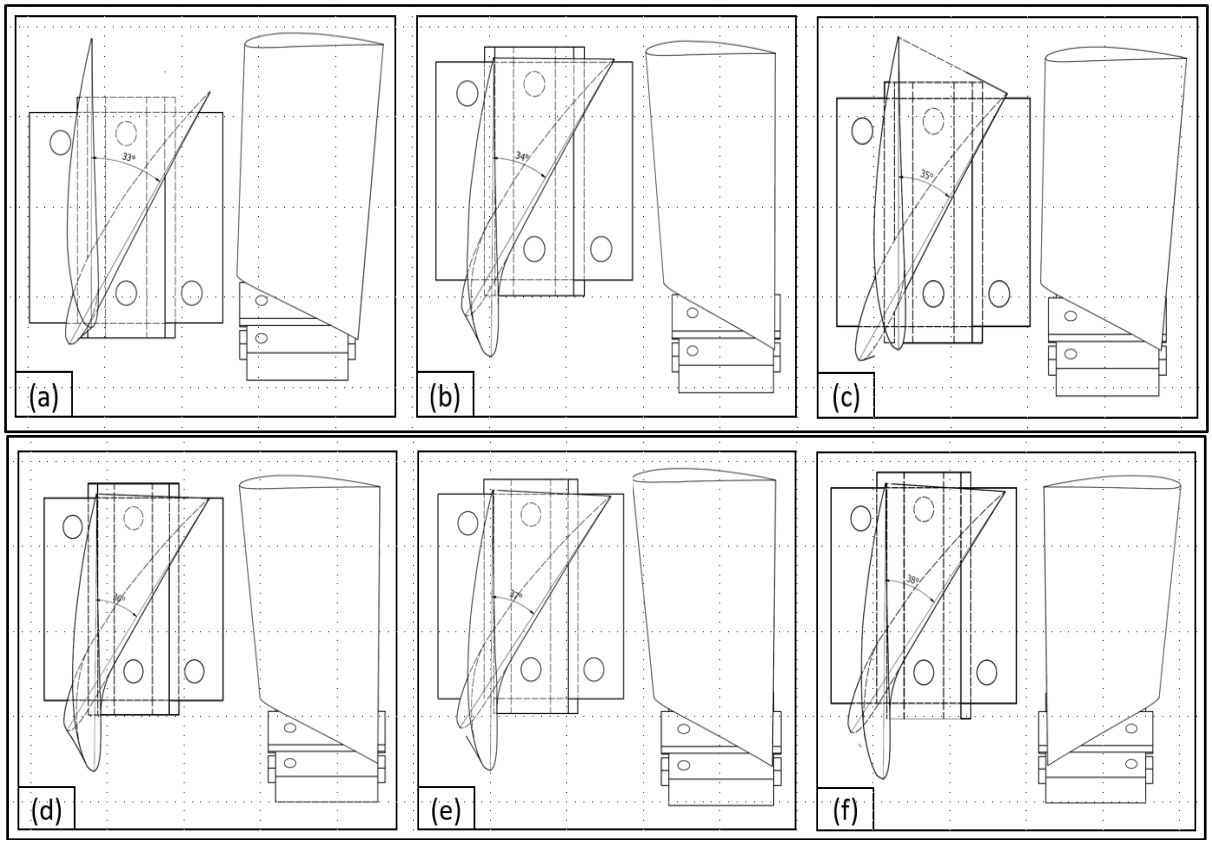

Fig. 2. Engineering Design of Steam Turbine Blade based on twist angle, (a) 33 Degree, (b) 34 Degree, (c) 35 Degree, (d) 36 Degree, (e) 37 Degree, (f) 38 Degree

2.2. Simulation

ANSYS is a widely used engineering simulation software that offers several types of simulations i.e. structural analysis, fluid dynamics, electromagnetic, explicit dynamics, multi physics and system simulation to analyse and optimize various physical phenomena. In this study the static structural, steady state thermal and fluent analysis have been implemented to simulate the optimal blade angle and other variables. Figure 3 below provides a visual representation of the geometrical design for better understanding.

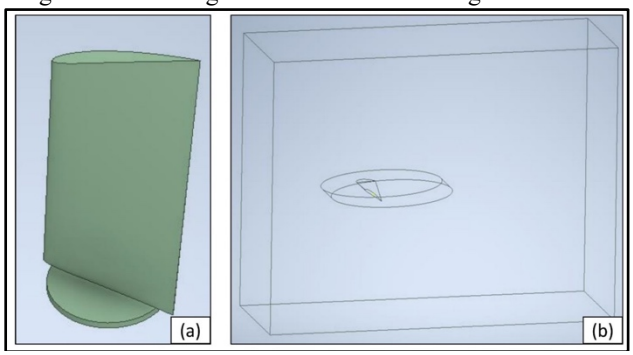

Fig. 3. The Geometrical Setup for Simulation, (a) Static and Thermal, (b) Fluent

Following the geometrical setup, the parameter must be set. Table 2 shows the parameter

Table 2. Parameter Setup for Simulation

Material	Aluminium Alloy
Body Sizing	$8x10^{(-4)}$
Rotational velocity	187,5 rad/s
Gravity	9,806 m/s^2
Inlet Pressure	49,25 kPa
Temperature	348,27 K
Outlet Pressure	0,0135Mpa

For additional parameter, In CFD Setup, there are several parameters that can be used to get an optimal outcome. It is recommended to conduct a convergence study in ANSYS simulations to attain superior quality. Convergence analysis is repeating the simulation with increasing mesh sizes or solver settings and comparing the results to assess the amount of convergence. When the results no longer noticeably alter as the mesh size or solver parameters are increased, the simulation is said to have converged. For Fluent only, the iterations are 6000x in order to get a good quality. The parameters are demonstrated in figure 4.

3. Result and Discussion

3.1. Static Structural

It simulates the structural behaviour of a system or component under static loads. This analysis is used to predict the stress,

strain, deformation, and failure of structures, components, and assemblies under steady-state loading conditions. The following steps are contained within ANSYS's static structural analysis. generation of geometry, meshing, material specification, solution, and post-processing. Further meshing can be sub-classified into mesh quality, mesh type, body sizing, etc. In this case, the quality of meshing is high, the mesh type is skewness, and the body sizing is $8x10^{(-4)}$. Figure 5 below shows the mesh metric's skewness value.

Solver	Type	Pressure-Based	
	Velocity Formulation	Absolute	
	Time	Steady	
Model	Viscous	Renormalization-group (RNG) k-epsilon, Standard Wall Functions	
Solution Methods	Pressure-Velocity Coupling Scheme	Simple	
	Spatial Discretization	Gradient	Least Squares Cell Based
		Pressure	PRESTO!
		Momentum	Second Order Upwind
		Volume Fraction	First Order Upwind
		Turbulent Kinetic Energy	First Order Upwind
Solution Controls	Under-Relaxation Factors	Pressure	0.3
		Density	1
		Body Forces	1
		Momentum	0.7
		Volume Fraction	0.5

Fig. 4. CFD Solver Parameter (Guodong Yi *, Huifang Zhou, Lemiao Qiu * and Jundi Wu, 2020)

For the mesh of a steam turbine blade, the allowable skewness ranges from 0.80 to 0.94 (see Figure 5).

Fig. 5. Skewness and Orthogonal Quality Mesh Spectrums

The static structural analysis calculated total deformation, stress and strain as shown in Table 3.

Table 3. Static Structural Result of Steam Turbine Blade

No.	Twist Angle	Total Deformation (mm)	Stress (MPa)	Strain (mm/mm)
1.	33	0.39	33.9	0.58
2.	34	0.44	42.77	0.83
3.	35	0.33	33.16	0.52
4.	36	0.39	46.45	0.79
5.	37	0.38	41.44	0.73
6.	38	0.39	40.05	0.69

The total deformation, stress, and strain is determined by using static structural simulation. Three spatial components often combine to generate total deformation. Strain is the result of a material deforming due to stress, while stress is a measure of what the substance experiences from externally applied pressures. The total deformation, stress and strain graph have been computed to find the optimal values. For the graph please refer to figure 7.

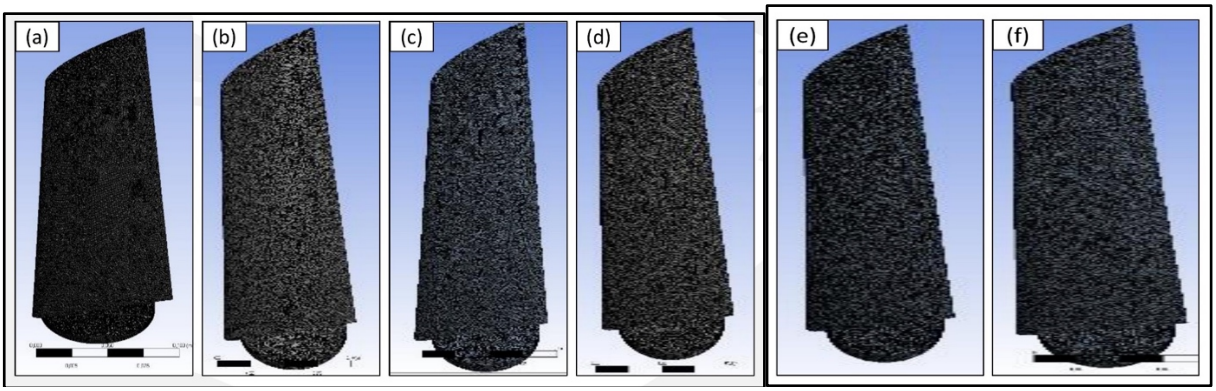

Fig. 6. The Meshing of Steam Turbine Blade, (a) 33, (b) 34, (c) 35, (d) 36, (e) 37, (f) 38 degree

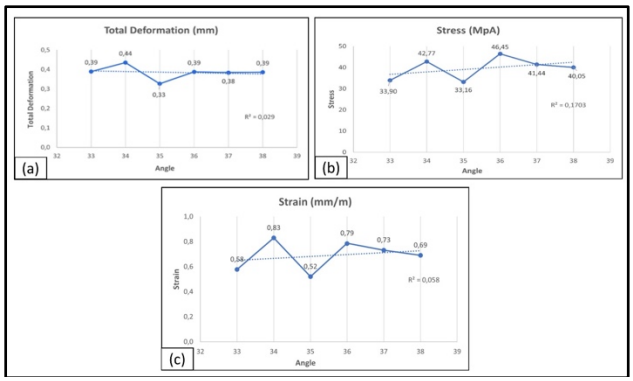

Fig. 7. The Graph Result of Static Structural, (a) Total Deformation, (b) Stress, (c) Strain

Based on simulations performed with varying blades angles of 33°, 34°, 35°, 36°, 37° and 38 ° degrees, the graph (a) configured the maximum total deformation of 0.44 mm at 34° and minimum total deformation of 0.33 mm at 35°. In graph (b) the minimum stress of 33.16 MpA at 35° twist angle and maximum stress of 46.45 MpA at 36° is being computed. The graph (c) depicts the minimum strain of 0.52 mm/min at 35° and maximum stain of 0.83 mm/min at 34°.

3.2. Steady-State Thermal

It is the type of analysis used to model the thermal behaviour of a structure or element under steady-state circumstances. The temperature distribution, heat transfer rates and thermal stresses is determined using this approach. The steady state thermal analysis performed using ANSYS consists of the succeeding phases. The creation of geometry, meshing, boundary conditions, material specifications, finding a solution, and post-processing. Further meshing is divided into mesh type, mesh quality, body size, etc. In this case, the body sizing is $8x10^{(-4)}$, mesh type is skewness and the mesh quality is high. Please refer to the Table 4

Table 4. Steady State Thermal Result of Steam Turbine Blade

No.	Twist Angle	Temperature (K)	Total Heat Flux (W/m^2)
1.	33	620	1.44E+08
2.	34	620	1.37E+08
3.	35	620	1.55E+08
4.	36	620	1.73E+08
5.	37	620	1.37E+08
6.	38	620	1.4E+08

A graph is drawn to represent the values and extract the conclusions. The graph is Figure 8.

Based on simulations performed with varying blade angles of 33º, 34º, 35º, 36º, 37º and 38 º degrees, the graph configured a decreasing trend at 34º, quite different from the Static structure, an increasing shift from 34º to 36º and again a decline at 37º. The graph shows the maximum heat flux of 1.73E+08 (W/m^2) at 36º and the lowermost 1.37E+08 (W/m^2) at 34º and 37º. The temperature graph is constant since each twist angle has the same temperature.

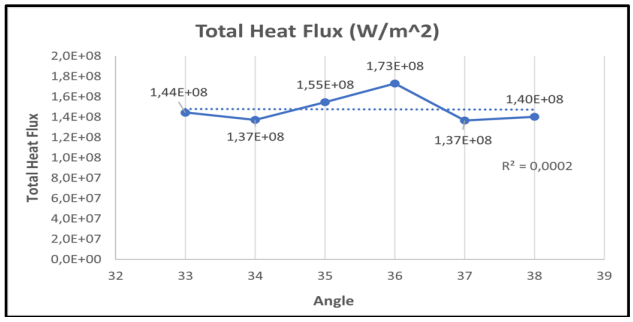

Fig. 8. Total Heat flux at the varying blade angles

3.3. Fluent Analysis

Lift, drag, average pressure, air velocity, and the highest temperature are all variables that is obtained through a fluent analysis. The meshing operation must first be carried out to obtain values. Mesh quality, mesh type, mesh size, body sizing, insulation, and other perimeters are all used in this method. In this situation, the meshing quality is high, the mesh type is skewness, the meshing size is ($1x10^{(-3)}$) and the body size is ($8x10^{(-4)}$). The meshing process velocity must be determined for the insulation. The value is determined to be $2\,^{m}/_{s}$ by the computation.

The result of the meshing operation is shown in Figure 9.

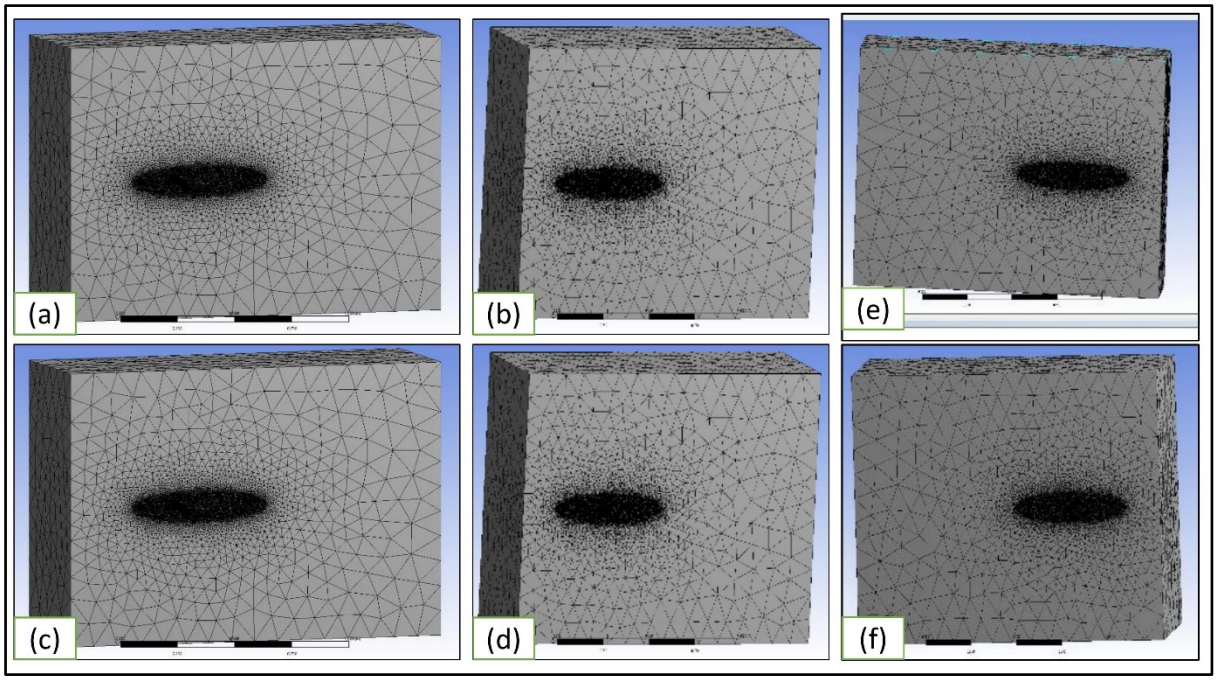

Fig. 9. The Mesh Result of Steam Turbine Blade, (a) 33, (b) 34, (c) 35, (d) 36, (e) 37, (f) 38 degrees

Fluent analysis of the meshing system determines lift, drag, average pressure, air velocity, and the maximum temperature variables. The outcome is shown in Table 5 below.

Table 5. Fluent Analysis Result of Steam Turbine Blade

No.	Twist Angle	Lift (N)	Drag (N)	Pressure Average (kPa)	Velocity of Air (m/s)	Pressure Maximum (kPa)
1.	33	457.31	140.41	26.36	376.48	60.27
2.	34	551.17	181.65	24.76	405.99	61.21
3.	35	507.65	170.16	26.19	383.97	61.41
4.	36	477.14	170.56	25.04	382.99	64.57
5.	37	462.11	177.99	25.88	380.6	61.91
6.	38	474.5	183.74	24.99	381.25	61.2

Two of the five values derived from fluent analysis are Lift and Drag. Lift and drag are the components of this force that are parallel to the flow direction and perpendicular to the incoming flow direction, respectively. As the blade's velocity is zero meters per second, a tool in CFD Post is implemented to get the air velocity. Finally, to get the pressure maximum employed the contour from CFD Post. Using the values from Table 5, the graph is being generated.

From the graph (a) it is deduced that at 33º the lift is 457.31 N, it reached to its peak point 551.17 N at 34º, and then gradually dropped to 474.5 N at 38º. In graph (b) the least value of drag is 140.41 N at 33º then it starts increasing to 181.65 N at 34º, then it descends again and the maximum drag

of 183.74 N calculated at 38º. In graph (c) the maximum pressure average of 26.36 is calculated at 33 and minimum of 24.76 at 34. In graph (d) the minimum velocity of air is 376.48 m/s at 33º and maximum at 405.99 m/s at 34º. The pressure maximum is plotted in graph (e) with least value of 60.27 at 33º and maximum value of 64.57 at 36º. The velocity magnitude, relative velocity magnitude and tangential velocity of stream turbine has been simulated with profiles in figure 11, 12 and 13 respectively.

Figure 12 and 13, shows the relative velocity magnitude and Tangential Velocity respectively.

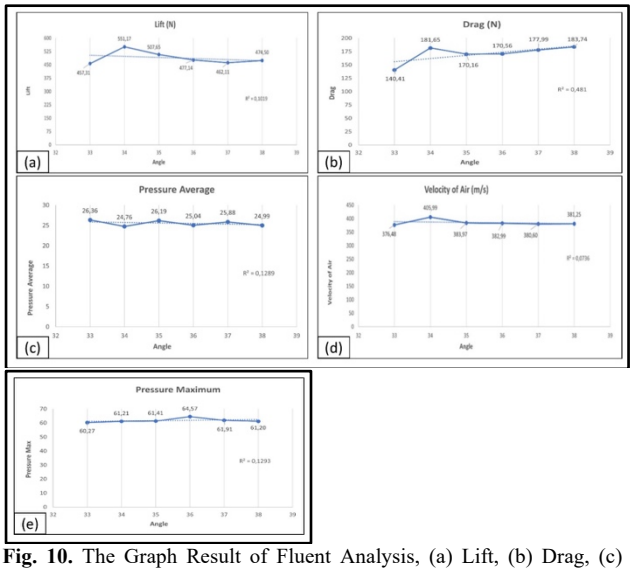

Fig. 10. The Graph Result of Fluent Analysis, (a) Lift, (b) Drag, (c) Pressure Average, (d) Velocity of Air, (e), Pressure Maximum

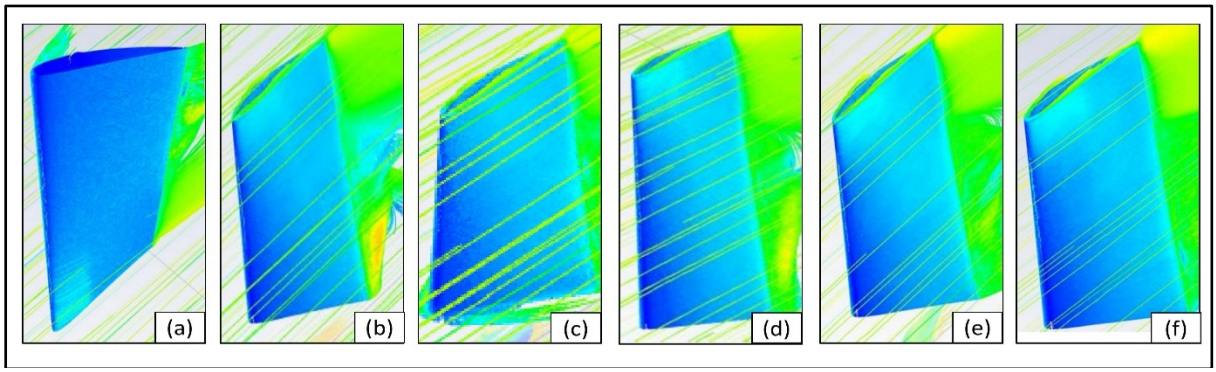

Fig. 11. Velocity Magnitude of Steam Turbine Blade, (a) 33, (b) 34, (c) 35, (d) 36, (e) 37, (f) 38 degrees

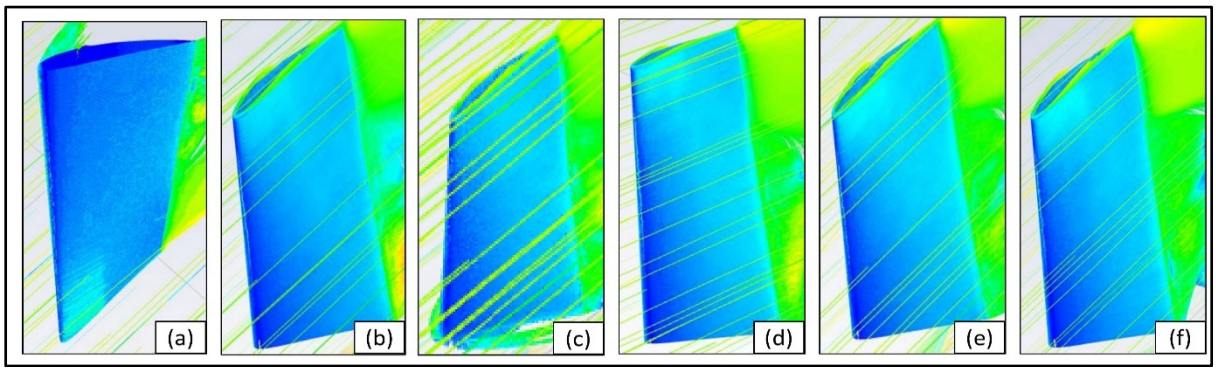

Fig. 12. Relative Velocity Magnitude of Steam Turbine Blade, (a) 33, (b) 34, (c) 35, (d) 36, (e) 37, (f) 38 degrees

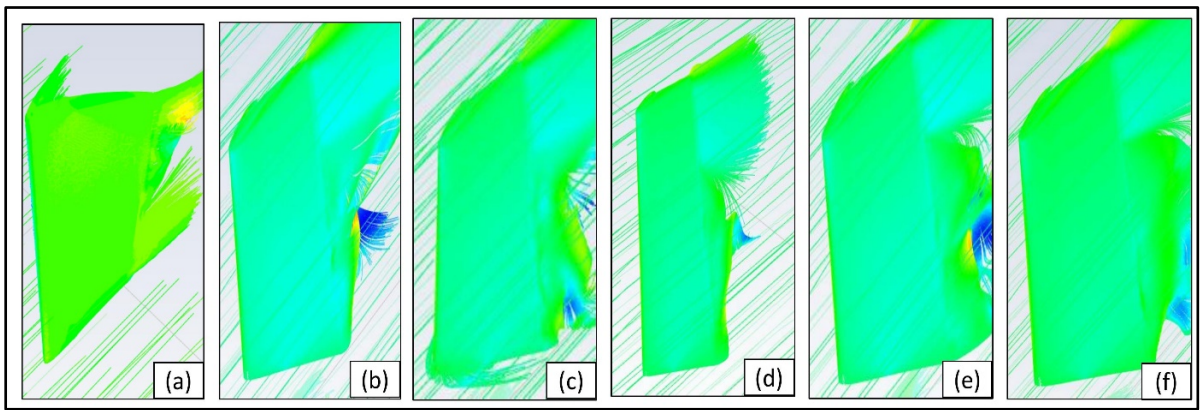

Fig. 13. Tangential Velocity of Steam Turbine Blade, (a) 33, (b) 34, (c) 35, (d) 36, (e) 37, (f) 38 degrees

4. Conclusions

In this study the three types of simulations i.e. static structural, steady state thermal and fluent analysis have been performed on the aluminium alloy steam turbine blades with varying blade angles of 33º, 34º, 35º, 36º, 37º and 38º. The following conclusions are drawn:

- Static Structural Analysis: In this investigation the lowest total deformation of 0.33 mm, minimum stress of 33.16 MpA and least stain of 0.52 mm/min has occurred at a tilt angle of 35º of turbine blade.
- Steady State Thermal: This simulated the maximum Total heat flux of 1.73E+08 (W/m^2) at 36º and the lowermost 1.37E+08 (W/m^2) at 34º and 37º. while the Total heat flux recorded at 35º is 1.55E+08 (W/m^2).
- Fluent Analysis: The lift, Drag, pressure average and velocity of air at the twist angle of 35º are 507.65 N, 170.16 N, 26.19 kPa and 383.97 m/s respectively.
- This finding also provides insight into the use of aluminium alloy as turbine blades, further more Aluminium Metal Matrix Composite can be doped with fillers to improve corrosion resistance.

In accordance with the results and findings, a stream turbine blade made of aluminium alloy should be tilted at a 35° for best performance. This study proposes the potential of aluminium alloy in the manufacturing of steam turbine blade. Future models of the turbine blade may possibly simulate other variables for a perfect match to the actual operating conditions.

Acknowledgment
The authors would like to express their gratitude to Hibah RKI 2023 under contract No. 2645/UN1/DITLIT/Dit-Lit/PT.01.03/2023.

References

[1] A. Mambro, F. Congiu, and E. Galloni, "Influence of stage design parameters on ventilation power produced by steam turbine last stage blades during low load operation," *Ther Sci Eng Progr*, vol. 28, p. 101054, Feb. 2022, doi: 10.1016/j.tsep.2021.101054.

[2] A. D. Nugraha *et al.*, "First-rate manufacturing process of primary air fan (PAF) coal power plant in Indonesia using laser powder bed fusion (LPBF) technology," *J Mater Res Techol*, vol. 18, pp. 4075–4088, May 2022, doi: 10.1016/j.jmrt.2022.04.056.

[3] P. J. Schubel, "Cost modelling in polymer composite applications: Case study – Analysis of existing and automated manufacturing processes for a large wind turbine blade," *Comp B: Eng*, vol. 43, no. 3, pp. 953–960, Apr. 2012, doi: 10.1016/j.compositesb.2011.11.036.

[4] R. H. Barnes, E. V. Morozov, and K. Shankar, "Improved methodology for design of low wind speed specific wind turbine blades," *Compos Struct*, vol. 119, pp. 677–684, Jan. 2015, doi: 10.1016/j.compstruct.2014.09.034.

[5] J. A. Rodríguez *et al.*, "Fatigue of steam turbine blades at resonance conditions," *Eng Fail Anal*, vol. 104, pp. 39–46, Oct. 2019, doi: 10.1016/j.engfailanal.2019.05.027.

[6] L. Kong *et al.*, "A near-zero energy system based on a kinetic energy harvester for smart ranch," *iScience*, vol. 25, no. 12, p. 105448, Dec. 2022, doi: 10.1016/j.isci.2022.105448.

[7] C. Pavese, T. Kim, and J. P. Murcia, "Design of a wind turbine swept blade through extensive load analysis," *Renew Ener*, vol. 102, pp. 21–34, Mar. 2017, doi: 10.1016/j.renene.2016.10.039.

[8] J. Lopes, D. Stefaniak, L. Reis, and P. P. Camanho, "Single lap shear stress in hybrid CFRP/Steel composites," *Proc Struct Integr*, vol. 1, pp. 58–65, 2016, doi: 10.1016/j.prostr.2016.02.009.

[9] E. Buechler *et al.*, "Global changes in electricity consumption during COVID-19," *iScience*, vol. 25, no. 1, p. 103568, Jan. 2022, doi: 10.1016/j.isci.2021.103568.

[10] R. Adi Himarosa, S. Dini Hariyanto, W. Hozaifa Hasan, and M. Akhsin Muflikhun, "Failure analysis of platen superheater tube, water wall tube, and sealpot plate: A case study from electricity power plant in indonesia," *Engin Fail Anal*, vol. 135, p. 106108, May 2022, doi: 10.1016/j.engfailanal.2022.106108.

[11] M. Thangamuthu *et al.*, "Polymer Photoelectrodes for Solar Fuel Production: Progress and Challenges," *Chem. Rev.*, vol. 122, no. 13, pp. 11778–11829, Jul. 2022, doi: 10.1021/acs.chemrev.1c00971.

[12] A. Al Noman *et al.*, "Savonius wind turbine blade design and performance evaluation using ANN-based virtual clone: A new approach," *Heliyon*, vol. 9, no. 5, p. e15672, May 2023, doi: 10.1016/j.heliyon.2023.e15672.

[13] A. Gantayet and D. K. Dheer, "A multi-objective optimisation strategy exploring the energy routing capability of a smart transformer while integrating hybrid energy hub into a distribution network," *Sustain Ener, Gr Netw*, vol. 32, p. 100956, Dec. 2022, doi: 10.1016/j.segan.2022.100956.

[14] M. Salvadori, P. Tudisco, D. Ranjan, and S. Menon, "Numerical investigation of mass flow rate effects on multiplicity of detonation waves within a H2/Air rotating detonation combustor," *International J Hydr Ener* vol. 47, no. 6, pp. 4155–4170, Jan. 2022, doi: 10.1016/j.ijhydene.2021.10.270.

[15] S. R. Paramati, U. Shahzad, and B. Doğan, "The role of environmental technology for energy demand and energy efficiency: Evidence from OECD countries," *Renew Sustain Ener Rev*, vol. 153, p. 111735, Jan. 2022, doi: 10.1016/j.rser.2021.111735.

[16] W. Wu, R. Yao, J. Wang, H. Su, and X. Wu, "Leading edge impingement cooling analysis with separators of a real gas turbine blade," *Appl Therm Engin*, vol. 208, p. 118275, May 2022, doi: 10.1016/j.applthermaleng.2022.118275.

[17] S. Andringa *et al.*, "Low-energy physics in neutrino LArTPCs," *J. Phys. G: Nucl. Part. Phys.*, vol. 50, no. 3, p. 033001, Jan. 2023, doi: 10.1088/1361-6471/acad17.

[18] S. Wu *et al.*, "Microstructure and mechanical properties of C Hf0.25NbTaW0.5 refractory high-entropy alloys at room and high temperatures," *J Mat Sci Techn*, vol. 97, pp. 229–238, Jan. 2022, doi: 10.1016/j.jmst.2021.05.015.

[19] W. Balasooriya, C. Clute, B. Schrittesser, and G. Pinter, "A Review on Applicability, Limitations, and Improvements of Polymeric Materials in High-Pressure Hydrogen Gas Atmospheres," *Pol Rev*, vol. 62, no. 1, pp. 175–209, Jan. 2022, doi: 10.1080/15583724.2021.1897997.

[20] J. Wen, L. Chen, X. Duan, J. Yang, Q. Liu, and L. Liu, "Fracture Failure Performance of 35VB Steel High-Strength Bolts Used in Subtropical Humid Climate," *J. Mater. Civ. Eng.*, vol. 33, no. 12, p. 04021359, Dec. 2021, doi: 10.1061/(ASCE)MT.1943-5533.0003971.

[21] S. M. A. Noori Rahim Abadi, A. Ahmadpour, S. M. N. R. Abadi, and J. P. Meyer, "CFD-based shape optimization of steam turbine blade cascade in transonic two phase flows," *Appl Therm Engin*, vol. 112, pp. 1575–1589, Feb. 2017, doi: 10.1016/j.applthermaleng.2016.10.058.

[22] Y. Triasdian, H. Pamingotan, B. Triatmodjo, R. Sriwijaya, M. Mahardika, and M. A. Muflikhun, "A Study Analysis of Micro-Hydro Powerplant (MHPP) Potential from Cooling of Steam Turbine," in *2020 International Conference on Technology and Policy in Energy and Electric Power (ICT-PEP)*, Bandung, Indonesia: IEEE, Sep. 2020, pp. 33–37. doi: 10.1109/ICT-PEP50916.2020.9249919.

[23] W. Li *et al.*, "Effects of embankment layouts on train aerodynamics in a wind tunnel configuration," *J W Eng Ind Aerod*, vol. 220, p. 104830, Jan. 2022, doi: 10.1016/j.jweia.2021.104830.

[24] Z. Duan, Q. Huang, and Q. Zhang, "Life cycle assessment of mass timber construction: A review," *Build Environ*, vol. 221, p. 109320, Aug. 2022, doi: 10.1016/j.buildenv.2022.109320.

[25] G. Yi, H. Zhou, L. Qiu, and J. Wu, "Hot Blade Shape Reconstruction Considering Variable Stiffness and Unbalanced Load in a Steam Turbine," *Energies*, vol. 13, no. 4, p. 835, Feb. 2020, doi: 10.3390/en13040835.

[26] M. Naseem, A. Saleem, and M. S. Naseem, "Investigation of blade design parameters for performance improvement of hydraulic cross flow turbine," *Oc Eng*, vol. 257, p. 111663, Aug. 2022, doi: 10.1016/j.oceaneng.2022.111663.

[27] J. Hu, X. Han, Y. Tao, and S. Feng, "A magnetic crawler wall-climbing robot with capacity of high payload on the convex surface," *Robot Auton Sys*, vol. 148, p. 103907, Feb. 2022, doi: 10.1016/j.robot.2021.103907.

[28] S. Rakhsha, M. Rajabi Zargarabadi, and S. Saedodin, "The effect of nozzle geometry on the flow and heat transfer of pulsed impinging jet on the concave surface," *Int J Ther Sci*, vol. 184, p. 107925, Feb. 2023, doi: 10.1016/j.ijthermalsci.2022.107925.

[29] T. Zhou, H. Cao, M. Zhang, and C. Liao, "Performance simulation of wind turbine with optimal designed trailing-edge serrations," *Energy*, vol. 243, p. 122998, Mar. 2022, doi: 10.1016/j.energy.2021.122998.

[30] B. Moynihan, B. Moaveni, S. Liberatore, and E. Hines, "Estimation of blade forces in wind turbines using blade root strain measurements with OpenFAST verification," *Ren Ener*, vol. 184, pp. 662–676, Jan. 2022, doi: 10.1016/j.renene.2021.11.094.

[31] A. Martin and F. Husaini, "Design, Manufacturing and Testing of Inversed Taper NACA 4412 Airfoil with Blade Made of Hybrid Empty Fruit Bunch Bio-composites," *JMechE*, vol. 19, no. 2, pp. 79–96, Apr. 2022, doi: 10.24191/jmeche.v19i2.19766.

[32] I. P. Okokpujie, L. K. Tartibu, K. Babaremu, C. Akinfaye, A. T. Ogundipe, and E. T. Akinlabi, "Study of the corrosion, electrical, and mechanical properties of aluminium metal composite reinforced with coconut rice and eggshell for wind turbine blade development," *Cl Eng Technol*, vol. 13, p. 100627, Apr. 2023, doi: 10.1016/j.clet.2023.100627.

.